Person Identification at a Distance via Ocular Biometrics

Aishwarya Jain, Paritosh Mittal, Gaurav Goswami, Mayank Vatsa, and Richa Singh
IIIT Delhi, India
{aishwarya10007, paritosh10059, gauravgs, mayank, rsingh}@iiitd.ac.in

Abstract

The performance of iris recognition reduces when the images are captured at a distance. However, such images generally contain periocular region which can be utilized for person recognition. In this research, we propose a novel context switching algorithm that dynamically selects the best descriptor for color iris and periocular regions. Using predefined protocols, the performance of the proposed algorithm is evaluated on UBIRIS V2 and FRGC datasets, and the results show improved performance compared to existing algorithms.

1. Introduction

Iris is considered to be one of the most discriminating biometric modality. Existing research primarily focuses on images captured in constrained environment where a near infrared imaging sensor acquires iris patterns at a distance of 10 to 30 centimeters. However, in several law enforcement applications, users are non-cooperative and images are typically obtained at larger distances. In such applications, the images acquired can be noisy and may be affected by variations in pose, illumination, occlusion due to eyelids, and specular reflections. Figure 1 shows sample of non-ideal images that are obtained in such environment. Recent results have shown that the performance of iris recognition is significantly affected in these unconstrained scenarios [13], [15]. Recent research is focusing on developing hardware and software solutions for iris recognition at a distance and in presence of such challenges. Sarnoff has designed an iris scanner which is capable of capturing iris image at a distance of up to 10 feet[1]. Park et al. [14] proposed periocular biometrics which focuses on discriminating features near the eye (ocular) region. Thereafter, several approaches were proposed to extend the state-of-art in ocular biometrics [3], [5], [6], [8], [10], [16], [18], [19], [24], [25], [26].

[1]http://www.sri.com/engage/products-solutions/iris-move-biometric-identification-systems

Figure 1: Iris images captured in unconstrained environment: (a) when periocular region is partially occluded, (b) when iris region is occluded due to closed eye lids, and (c) when both iris and periocular regions are blurred.

This paper presents a novel approach of quality based context switching between features for both color iris and periocular regions. While *context switching* is not new in biometrics [22], [23], the proposed approach, to the best of our knowledge, is the first that combines color iris and periocular information and switches between different iris and periocular features (descriptors). Switching between descriptors is required because each periocular image may contain a different type of noise; therefore, utilizing a single descriptor for all images may not be optimal. Hence, depending on the *quality* of the image, an appropriate descriptor can be employed to extract features. The performance of the proposed approach is evaluated with quality based context switching among three descriptors: Local Binary Pattern (LBP) [11], GIST [12], and Scale Invariant Feature Transform (SIFT) [7]. The experiments conducted on the UBIRIS v2 and FRGC databases using the protocol propose by Tan and Kumar [19] indicate that the proposed algorithm achieves state-of-the-art results. The results also show that the proposed approach is robust in non-ideal scenarios when one of the biometric modalities is of poor quality.

2. Quality based Context Switching and Fusion of Periocular and Iris Biometrics

The proposed algorithm is developed based on the premise that in non-ideal (at a distance) capture conditions, images suffer due to poor quality. It is our assertion that any one quality enhancement or recognition al-

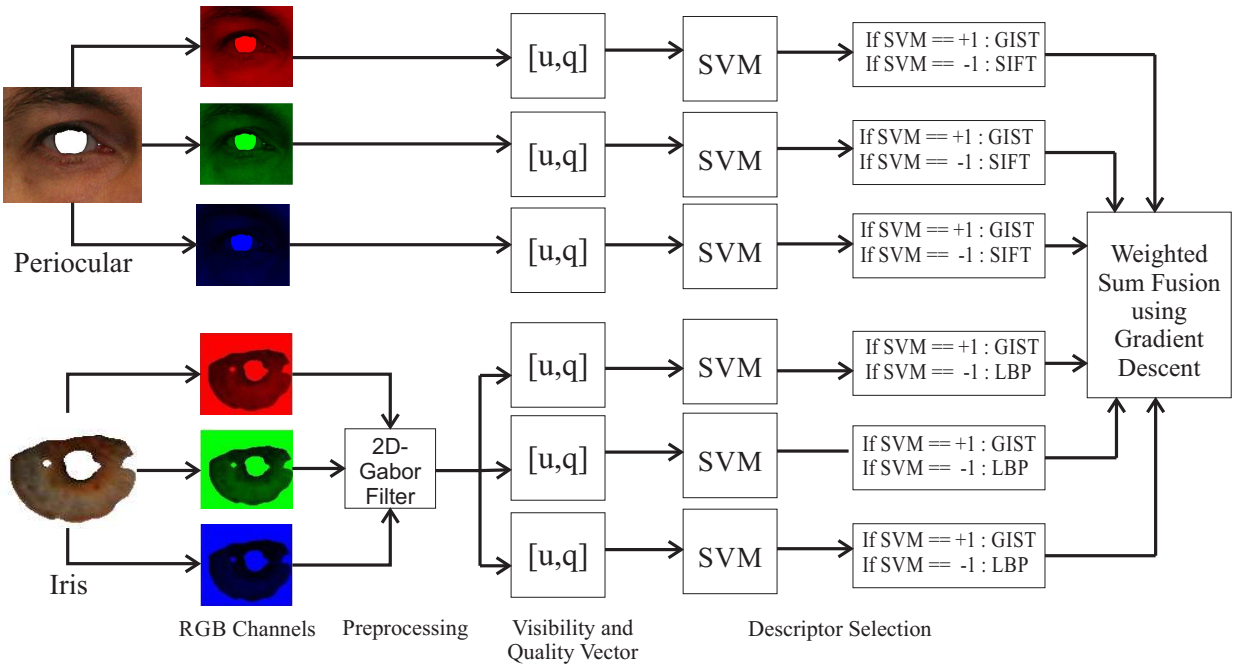

Figure 2: Steps involved in the proposed context switching based periocular recognition algorithm.

gorithm cannot suffice for achieving optimum performance in such conditions [17]. Furthermore, in some cases, one feature/modality may provide better results than the other and in a different condition, the optimum choice of feature/modality may change. Therefore, the proposed algorithm utilizes a context switching approach to determine the optimum choice dynamically at runtime. Figure 2 illustrates the steps involved in the proposed quality-based context switching algorithm. The algorithm utilizes color iris and periocular images for identity recognition and consists of the following steps: preprocessing, quality assessment, context switching among iris and periocular descriptors, and recognition. These individual steps are detailed below:

Preprocessing: The ocular image that contains both iris and periocular regions is resized to 150 $\times$ 120. First, iris and periocular regions are separated using an existing segmentation algorithm [19]. The two biometric modalities are then extracted so that these can be processed individually.

Let I^i_{iris} be the color iris image and I^i_{peri} be the color periocular image, where $i \in R, G, B$ represents the three color channels. Since the iris region can be noisy, a Gabor filter [4] is used to remove noise, enhance the features, and smoothen the image. As shown in Equation (1), a Gabor filter [4] is applied on I^i_{iris}. While this operator can be applied on periocular regions as well, databases used in this research have good quality periocular regions and therefore applying filtering on periocular images only increases the computational overhead.

$$X^i_{iris-j} = G_j * I^i_{iris} \tag{1}$$

Here, $*$ denotes the convolution operator and G_j represents the Gabor filter with central frequencies and variances as parameters. With j Gabor filters, X^i_{iris-j} is computed and the average response is calculated for each color channel:

$$X^i_{iris-a} = \sum_j X^i_{iris-j} \tag{2}$$

Visible Area and Quality Score: Both periocular and iris images may be affected by different types of irregularities or quality factors. Depending on the quality of the input image, the performance of descriptors can also vary. Therefore, the proposed context switching algorithm is based on two quality measures, visible area and image quality, that are extracted using the iris and periocular images. Researchers have studied the performance of different descriptors such as Local Binary Pattern (LBP) [11], GIST [12] and Scale Invariant Feature Transform (SIFT) [7] on ocular recognition [3], [19]. Existing literature indicates that GIST is able to encode discriminative features even when camera-object distance is over four meters [3]. The combination of GIST and LBP has been found to provide good results for iris recognition at a distance whereas, the combination of SIFT and GIST yield better performance for periocular region. To determine the optimal combination of descriptors, we first estimate the visibility and quality factors of periocular and iris images.

Let $V(\cdot)$ be the visibility function which takes an image as input and outputs a quantized visibility score, u, in the range of [0,1]. From the input image, iris region is segmented using the segmentation algorithm proposed in [19]. The number of segmented iris pixels constitutes to the visibility score of iris whereas the remaining constitute the visibility score of periocular region. The score is calculated as the number of usable iris pixels divided by the total number of pixels in the image.

$$u^i_{iris} = V(X^i_{iris-a}) \qquad (3)$$
$$u^i_{peri} = V(I^i_{peri})$$

The quality score for iris and periocular images are computed using the redundant discrete wavelet transform approach (RDWT) based quality assessment algorithm proposed by Vatsa et al. [21]. The input image is decomposed into 3-level RDWT and energy of every sub-band is calculated. The quality factors of every sub-band are combined to compute the final quality score of the image.

$$q^i_{iris} = W(X^i_{iris-a}) \qquad (4)$$
$$q^i_{peri} = W(I^i_{peri})$$

Here, $W(\cdot)$ represents the quality function which takes an image as input and outputs a quality value in the range of [0,1]. The usability and quality scores are concatenated to compute one feature vector for iris and another for periocular image according to Equations 5 and 6.

$$F^i_{iris} = [u^i_{iris}; q^i_{iris}] \qquad (5)$$
$$F^i_{peri} = [u^i_{peri}; q^i_{peri}] \qquad (6)$$

Since the images are captured as color images in visible spectrum, there are three channels available in both iris and periocular images. Since some noise may be more prominent in particular color channels, we individually evaluate the quality and usability of the three channels. F_{iris} and F_{peri} thus denote a set of three feature vectors for the iris and periocular images (one pertaining to each channel, i.e., red, green, and blue).

Context Switching: The proposed context switching is performed based on image quality and information content. Therefore, depending on the color channel and feature descriptors (GIST, SIFT, and LBP), a combination of descriptors can be selected for a given color channel. This selection is learned using Support Vector Machine (SVM) [20] which performs a two-class classification based on the visible area and quality scores. A total of six SVM models are trained, three SVM models are trained for the R, G, and B channels of iris images and three SVM models for the periocular images (R,G,B channels). As shown in Equations 7 and 8 respectively, for iris images, SVM performs the selection between GIST and LBP descriptors whereas for periocular images, SVM predicts the use of GIST and SIFT feature descriptors.

$$S^i_{iris} = \begin{cases} GIST & \text{if } SVM(F^i_{iris}) = +1 \\ LBP & \text{if } SVM(F^i_{iris}) = -1 \end{cases} \qquad (7)$$

$$S^i_{peri} = \begin{cases} GIST & \text{if } SVM(F^i_{peri}) = +1 \\ SIFT & \text{if } SVM(F^i_{peri}) = -1 \end{cases} \qquad (8)$$

Depending on the output of SVM, appropriate descriptors are applied on individual channels of iris and periocular images and matched using χ^2 distance metric. S^i_{iris} and S^i_{peri} represent the match scores of iris and periocular image respectively. The similarity scores between probe and gallery images are computed using χ^2 distance metric and combined to produce a six-dimensional score vector according to Equation 9.

$$S = [S^i_{iris}; S^i_{peri}] \forall i \in \{R, G, B\} \qquad (9)$$

Recognition: Once the score vectors is obtained, they are combined using the weighted score fusion approach.

$$Score = \sum_{j=1}^{j=6} Z_j * S_j \qquad (10)$$

Here, Z_j are the weights associated with S_j where $j = \{1, 2, 3, 4, 5, 6\}$. Optimal values for these weights are learned using the gradient descent approach during training [2]. The fused score Z_j provides a similarity measure between a given probe image and a gallery image. For one probe image, these scores are computed for each subject in the gallery and recognition is performed by *identification-in-verification* mode.

3. Experimental Results

The performance of the proposed algorithm is evaluated on the publicly available UBIRIS V2 [15] and FRGC databases [1]. The images from the databases are acquired from a distance in the visible spectrum. All the experiments are performed using the identification protocol mentioned by Tan and Kumar [19]. The protocol and database are briefly discussed below:

1. **UBIRIS V2**: A subset of the UBIRIS V2 [15] is chosen that consists of 1000 images pertaining to 171 subjects. Out of these 1000 images, 96 images of 19 subjects are used for training whereas 904 images of the remaining subjects are used for testing. Ground truth

Descriptors Combination	Context Switching	Fusion Type	Accuracy (%)
Iris (LBP, GIST) + Peri (LBP, GIST)	LDA	LDA	17.3
Iris (LBP, GIST) + Peri (LBP, GIST)	SVM	LDA	20.2
Iris (LBP, GIST) + Peri (LBP, GIST)	LDA	SVM	54.3
Iris (LBP, GIST) + Peri (LBP, GIST)	SVM	SVM	52.1
Iris (LBP, GIST) + Peri (LBP, GIST)	LDA	Weighted Sum	70.3
Iris (LBP, GIST) + Peri (LBP, GIST)	SVM	Weighted Sum	65.2
Iris (SIFT, GIST) + Peri (SIFT, GIST)	LDA	LDA	35.6
Iris (SIFT, GIST) + Peri (SIFT, GIST)	SVM	LDA	49.3
Iris (SIFT, GIST) + Peri (SIFT, GIST)	LDA	SVM	60.8
Iris (SIFT, GIST) + Peri (SIFT, GIST)	SVM	SVM	59.8
Iris (SIFT, GIST) + Peri (SIFT, GIST)	LDA	Weighted Sum	65.3
Iris (SIFT, GIST) + Peri (SIFT, GIST)	SVM	Weighted Sum	68.8
Iris (SIFT, GIST) + Peri (LBP, GIST)	LDA	LDA	22.5
Iris (SIFT, GIST) + Peri (LBP, GIST)	SVM	LDA	33.7
Iris (SIFT, GIST) + Peri (LBP, GIST)	LDA	SVM	67.7
Iris (SIFT, GIST) + Peri (LBP, GIST)	SVM	SVM	63.1
Iris (SIFT, GIST) + Peri (LBP, GIST)	LDA	Weighted Sum	72.6
Tan & Kumar [19]	63.0 %		
Proposed (Iris (GIST, LBP) + Peri (SIFT, GIST))	SVM	Weighted Sum	75.4

Table 1: Rank-10 identification accuracy (%) on the UBIRIS V2 database.

of the dataset is manually annotated by humans where each pixel is appropriately marked as belonging to the iris or periocular regions. More details of the experimental protocol are available in [19].

2. **FRGC**: A subset of the FRGC database [1] is chosen that consists of 540 images pertaining to 163 subjects. Out of these 540 images, 40 images belonging to 13 subjects are utilized for training, whereas the remaining 500 images belonging to 150 subjects are utilized for testing. The publicly available source code provided by Tan and Kumar [19] is utilized to segment the image at a distance into iris and periocular regions.

To evaluate the efficacy of the proposed context switching and fusion framework, the performance is compared when (a) LDA [9] is utilized instead of SVM to predict the optimal descriptors and (b) when weighted sum rule fusion is replaced by SVM and linear discriminant analysis for computing the final match score. The key observations are discussed below:

- Figure 3 presents the results of descriptors on individual color channels of both iris and periocular recognition. As shown in Figure 3(a), GIST feature descriptor [12] yields the rank-10 identification accuracy of 48% for iris recognition which is better than both SIFT [7] and LBP [11]. GIST also outperforms other descriptors for periocular images.

- As shown in Figure 3(c), combining both iris and periocular for individual descriptors provides an improvement of 3%, 6% and 5% at rank-10 for SIFT, LBP and GIST respectively. This shows that fusion of iris and periocular improves the performance over either of them considered one at a time.

- For context switching, two classifiers are explored: SVM (support vector machines) and LDA. On the UBIRIS v2 database, as shown in Table 1, we observed that SVM outperforms LDA by 3%.

- Three score fusion techniques are used in the experiment namely, SVM, LDA, and weighted sum. Weighted sum rule yields the highest identification accuracy followed by SVM and LDA, irrespective of the context switching classifier (Table 1).

- By utilizing the two best performing descriptors for each biometric modality, context switching yields the best result of approximately 75% rank-10 identification accuracy. On the UBIRIS v2 database, as shown in Table 1, using SVM for switching and gradient descent weighted sum rule for fusion provides the best results as compared to other combinations. Similar results are observed for the FRGC database.

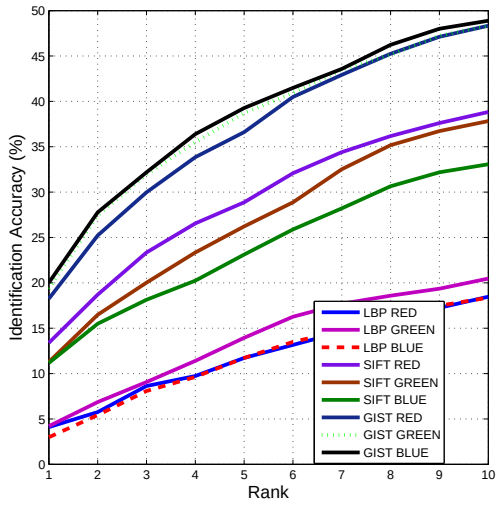

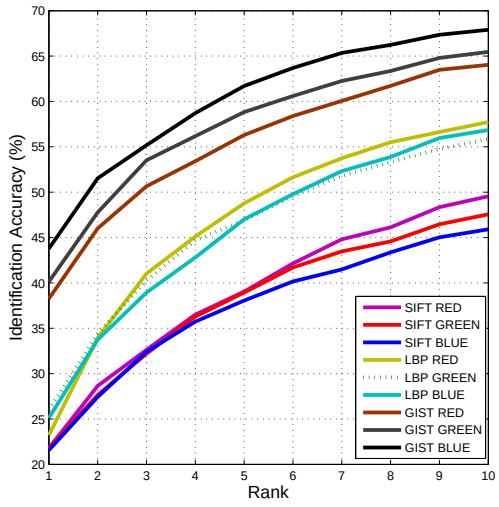

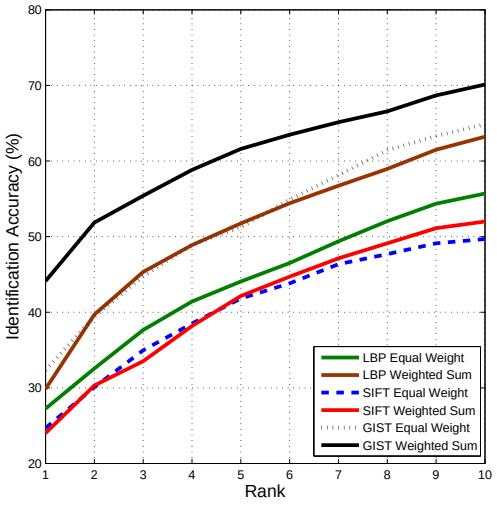

Figure 3: CMC curves on the UBIRIS V2 database with (a) iris recognition, (b) periocular recognition, and (c) fusion of individual descriptors.

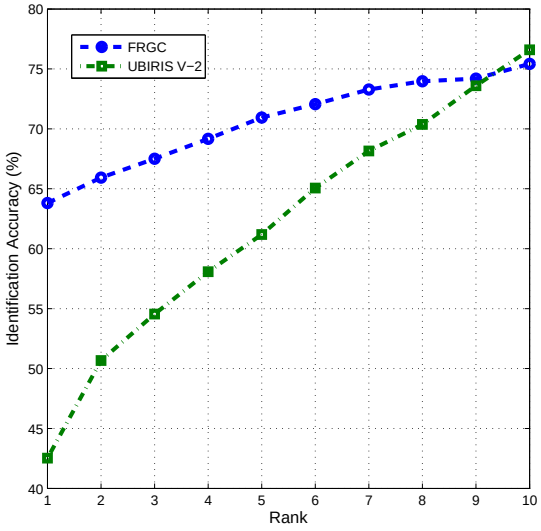

Figure 4: CMC curves of the proposed algorithm on the FRGC and UBIRIS v2 databases.

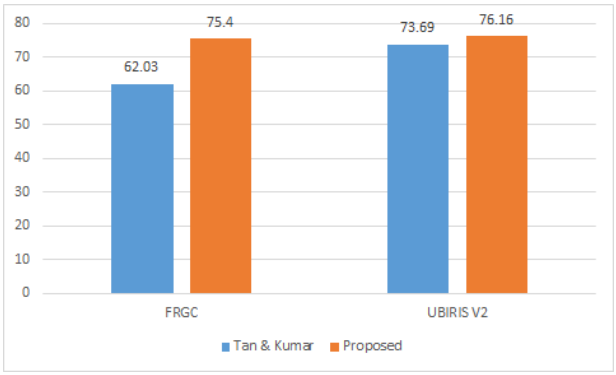

Figure 5: Rank-10 identification accuracy of the proposed algorithm on the FRGC and UBIRIS v2 databases.

- Figure 4 shows the cumulative match curves of the proposed algorithm on both FRGC and UBIRIS v2 databases. The performance of the proposed algorithm are compared with Tan and Kumar's [19] approach with the same experimental protocol and are summarized in Figure 5. The results show that the proposed algorithm is at least 12% better on the UBIRIS V2 database and around 2.4% better on the FRGC database.

- Computationally, the time taken to process one input image in identification mode is 28.14 seconds for UBIRIS V2 dataset on a system with 3 GHz quad core processor and 8 GB RAM in MATLAB programming environment.

4. Conclusion

With the increasing popularity of iris as a biometric modality, the requirement of iris recognition at a distance has become an important research problem, especially for law enforcement applications. Existing research combines fixed feature descriptors of iris and periocular images to determine the identity which may not be the optimal solution for all types of image quality and information content. This research presents an algorithm that is based on context switching of descriptors depending on the quality of iris and periocular images. It uses quality and visibility features to decide the optimal combination for a given input at runtime. Experimental results on the UBIRIS v2 and FRGC databases suggest that context switching helps in improving the identification accuracy compared to individual iris as well as periocular recognition. As a future research, we plan to extend this work for recognizing iris images captured at distance via mobile images.

5. Acknowledgements

We would like to thank Chun-Wei Tan and Dr. A. Kumar for sharing their segmentation code. We would also like to thank Dr. H. Proenca for providing the UBIRIS v2 database. This research is supported through a grant from Department of Electronics and Information Technology, Government of India, India.

References

[1] FRGC database. http://www.nist.gov/itl/iad/ig/frgc.cfm. [Online].

[2] J. Basak, K. Kate, V. Tyagi, and N. Ratha. A gradient descent approach for multi-modal biometric identification. In *ICPR*, pages 1322–1325, 2010.

[3] S. Bharadwaj, H. S. Bhatt, M. Vatsa, and R. Singh. Periocular biometrics: When iris recognition fails. In *BTAS*, 2010.

[4] J. G. Daugman. High confidence visual recognition of persons by a test of statistical independence. *IEEE TPAMI*, 15(11):1148–1161, 1993.

[5] V. Gottemukkula, S. K. Saripalle, S. P. Tankasala, R. Derakhshani, R. Pasula, and A. Ross. Fusing iris and conjunctival vasculature: Ocular biometrics in the visible spectrum. In *HST*, pages 150–155, 2012.

[6] A. Kumar and A. Passi. Comparison and combination of iris matchers for reliable personal authentication. *Pattern Recogn.*, 43(3):1016–1026, 2010.

[7] D. G. Lowe. Distinctive image features from scale-invariant keypoints. *IJCV*, 60(2):91–110, 2004.

[8] G. Mahalingam and K. Ricanek Jr. LBP-based periocular recognition on challenging face datasets. *EURASIP JIVP*, 2013(1):1–13, 2013.

[9] A. M. Martínez and A. C. Kak. PCA versus LDA. *IEEE TPAMI*, 23(2):228–233, 2001.

[10] H. Mehrotra, M. Vatsa, R. Singh, and B. Majhi. Biometric match score fusion using RVM: A case study in multi-unit iris recognition. In *CVPRW*, pages 65–70, 2012.

[11] T. Ojala, M. Pietikainen, and T. Maenpaa. Multiresolution gray-scale and rotation invariant texture classification with local binary patterns. *IEEE TPAMI*, 24(7):971–987, 2002.

[12] A. Oliva and A. Torralba. Modeling the shape of the scene: A holistic representation of the spatial envelope. *IJCV*, 42(3):145–175, 2001.

[13] C. N. Padole and H. Proenca. Periocular recognition: Analysis of performance degradation factors. In *ICB*, pages 439–445, 2012.

[14] U. Park, R. Jillela, A. Ross, and A. K. Jain. Periocular biometrics in the visible spectrum. *IEEE TIFS*, 6(1):96–106, 2011.

[15] H. Proenca, S. Filipe, R. Santos, J. Oliveira, and L. A. Alexandre. The UBIRIS-V2: A database of visible wavelength iris images captured on-the-move and at-a-distance. *IEEE TPAMI*, 32(8):1529–1535, 2010.

[16] A. Ross, R. Jillela, J. M. Smereka, V. N. Boddeti, B. V. Kumar, R. Barnard, X. Hu, P. Pauca, and R. Plemmons. Matching highly non-ideal ocular images: An information fusion approach. In *ICB*, pages 446–453, 2012.

[17] R. Singh, M. Vatsa, and A. Noore. Improving verification accuracy by synthesis of locally enhanced biometric images and deformable model. *Signal Processing*, 87(11):2746–2764, 2007.

[18] C.-W. Tan and A. Kumar. Human identification from at-a-distance images by simultaneously exploiting iris and periocular features. In *ICPR*, pages 553–556, 2012.

[19] C.-W. Tan and A. Kumar. Towards online iris and periocular recognition under relaxed imaging constraints. *IEEE TIP*, 22(10):3751–3765, 2013.

[20] V. N. Vapnik. *The Nature of Statistical Learning Theory*. Springer, 1995.

[21] M. Vatsa, R. Singh, and A. Noore. Integrating image quality in 2nu-svm biometric match score fusion. *IJNS*, 17(5):343–351, 2007.

[22] M. Vatsa, R. Singh, and A. Noore. Unification of evidence-theoretic fusion algorithms: A case study in level-2 and level-3 fingerprint features. *IEEE TSMC, Part A*, 39(1):47–56, 2009.

[23] M. Vatsa, R. Singh, A. Noore, and A. Ross. On the dynamic selection of biometric fusion algorithms. *IEEE TIFS*, 5(3):470–479, 2010.

[24] M. Vatsa, R. Singh, A. Ross, and A. Noore. Quality-based fusion for multichannel iris recognition. In *ICPR*, pages 1314–1317, 2010.

[25] D. L. Woodard, S. Pundlik, P. Miller, R. Jillela, and A. Ross. On the fusion of periocular and iris biometrics in non-ideal imagery. In *ICPR*, pages 201–204, 2010.

[26] V. Yano, A. Zimmer, and L. L. Ling. Multimodal biometric authentication based on iris pattern and pupil light reflex. In *ICPR*, pages 2857–2860, 2012.